EES Catalysis

COMMUNICATION

View Article Online
View Journal

Cite this: DOI: 10.1039/d4ey00261j

Received 1st December 2024,
Accepted 5th December 2024

DOI: 10.1039/d4ey00261j

rsc.li/eescatalysis

Selective electroreduction of CO_2 to formate by a heterogenized Ir complex using H_2O as an electron/hydrogen source†

Jieun Jung, *[a] Keun Woo Lee, ‡[a] Naonari Sakamoto, ‡[b] Selvam Kaliyamoorthy, ‡[a] Taku Wakabayashi, [a] Kenji Kamada, [a] Keita Sekizawa, [b] Shunsuke Sato, [b] Tomiko M. Suzuki, [b] Takeshi Morikawa [b] and Susumu Saito *[ac]

A newly synthesized tetradentate PNNP-coordinated iridium (Ir) complex, Mes-IrPPh2, immobilized on a carbon material, was found to be a superior catalyst for CO_2 electrochemical reduction reaction (CO_2ERR) to give formate, ($HCOO^-$), allowing an operation near the theoretical potential (−0.18 V *vs.* RHE, pH = 7.3) in water. The combined [Mes-IrPPh2] electrode furnished $HCOO^-$ with a current density of greater than 2.2 to 7.7 mA cm^{-2} over −0.27 to −0.47 V *vs.* RHE, providing faradaic efficiencies (FE) of >90%. The outstanding robustness of the electrode attained continuous production of $HCOO^-$ up to 12.5 mmol with 2.86 μmol of Mes-IrPPh2 at −0.27 V *vs.* RHE over 168 h. Furthermore, solar-driven electrochemical CO_2 reduction to $HCOO^-$ was also carried out in water with a Ni/Fe–Ni foam anode as a water oxidation catalyst and a silicon photovoltaic cell to achieve a solar-to-formate conversion efficiency (η_{STF}) of 13.7%.

Broader context

The electrochemical reduction of carbon dioxide (CO_2) has emerged as a crucial strategy for reducing global carbon emissions and advancing sustainable energy solutions. Utilizing water as an electron donor for CO_2 fixation offers a practical approach, particularly in the realm of renewable energy storage. Enhancing CO_2 reduction efficiency can be achieved through the heterogenization of molecular catalysts onto electrode surfaces. However, a significant challenge remains: the long-term durability of electrochemical CO_2 reduction in aqueous solutions, which often deteriorates after only a few hours. In this study, we present a novel Ir complex immobilized on a carbon material electrode to achieve both efficient and durable CO_2 reduction. The heterogenization of the Ir complex notably reduces the overpotential and yields formate as the main product with a high faradaic efficiency. Remarkably, the catalyst maintains its activity for a week, demonstrating exceptional long-term stability. It is worth noting here that, when the Ir electrode was employed in solar-driven electrochemical CO_2 reduction, the solar-to-formate conversion efficiency of 13.7% was achieved, highlighting its potential for scalable practical/industrial applications.

Introduction

The electrochemical reduction of carbon dioxide (CO_2) has received significant attention in recent years due to the growing demand for carbon-neutral energy carriers for the storage of renewable energy.[1] Reduction of CO_2 by utilizing water as an electron/hydrogen donor for the fixation of CO_2 is an ideal process for practical use. Thus, the development of catalysts for CO_2 reduction in aqueous solutions is the key to realizing this noble technology.[2] Various materials, including semiconductors and molecular metal complexes, have been studied for photoelectrochemical[3,4] and electrochemical[5–7] reduction of CO_2 to desired materials such as carbon monoxide (CO), formic acid, methanol, methane, and C_2+ compounds. Despite substantial efforts on the development of the CO_2 electrochemical reduction reaction (CO_2ERR), (i) low energetic efficiency requiring a large overpotential, (ii) poor selectivity for carbonaceous products in water originating from low solubility of CO_2, (iii) the competitive hydrogen evolution reaction (HER) and (iv) deactivation of the catalysts restrict this technology from practical use.[8]

Heterogenization of molecular catalysts on electrode surfaces has emerged as a promising approach in terms of lower catalyst loading and improving electron transfer efficiency.[9,10] Significant progress has been made in the functionalization of carbon surfaces of electrodes to anchor molecular catalysts as CO_2ERR electrocatalysts.[11–13] However, in many cases, the CO_2ERR in an aqueous solution halted after no more than a few hours, and thus, its long-term durability has remained a significant challenge. Solar-driven CO_2 conversion to formate

[a] Department of Chemistry, Graduate School of Science, Nagoya University, Chikusa, Nagoya 464-8602, Japan. E-mail: jung.jieun.z7@f.mail.nagoya-u.ac.jp
[b] Toyota Central R&D Laboratories, Inc, Nagakute 480-1192, Japan
[c] Integrated Research Consortium on Chemical Science (IRCCS), Nagoya University, Chikusa, Nagoya 464-8602, Japan. E-mail: saito.susumu.c4@f.mail.nagoya-u.ac.jp

† Electronic supplementary information (ESI) available. See DOI: https://doi.org/10.1039/d4ey00261j

‡ These authors contributed equally to this work.

($HCOO^-$) has also been carried out to achieve electrochemical CO_2 reduction using heterogenized metal complexes in combination with photovoltaic cells.[14–20] Although their solar-to-electricity conversion efficiencies are usually lower than those of the GaAs-based photovoltaic cells, silicon is known to be a more suitable material for photovoltaic cells owing to their higher cost performance. To improve solar-to-formate conversion efficiency, the cell voltage between the two poles must be reduced, and it is essential to develop an efficient electrocatalyst that can operate at a very low overpotential.

We recently reported tetradentate PNNP-coordinated iridium ((PNNP)Ir) complexes as efficient and robust photocatalysts to selectively reduce CO_2 to formic acid with high reactivity in an organic solvent (with a small amount of H_2O).[21,22] Herein, the Ir complexes were successfully exploited to catalyze CO_2 reduction in an aqueous solution through its heterogenization onto the surface of a carbon material electrode supported by carbon black and a polymer matrix.[23] This heterogenized Ir complex deployed on the carbon electrode is abbreviated as [Ir-ink] in this report, wherein (1) as depicted in Scheme 1, CO_2ERR at a very small overpotential of around 90 mV was achieved over the [Ir-ink] electrode (cathode) together with a platinum wire (anode) and Ag/AgCl as the counter and reference electrodes, respectively. The [Ir-ink] electrode exhibited outstanding CO_2 reduction activity with a current density of 2.2 mA cm^{-2} at −0.27 V *vs.* RHE. $HCOO^-$ was produced as the main product with a high faradaic efficiency (FE) of >98% in 1 h and prolonging the reaction time to 168 h with optimal conditions generated a total amount of 12.5 mmol of $HCOO^-$ (using *ca.* 2.86 μmol of Ir in [Ir-ink]). (2) The developed [Ir-ink] successfully promoted electrochemical CO_2 reduction to $HCOO^-$ utilizing H_2O as an electron and proton source in a two-compartment cell combined with photovoltaic (PV) cells. The solar-to-formate conversion efficiency (η_{STF}) reached 13.7% by combination with a Ni/Fe–Ni foam anode and a silicon PV cell.

Results and discussion

The (PNNP)Ir complexes were synthesized based on the previous reports[22,24] and Scheme S1, ESI.† [Ir-ink] electrodes were fabricated by drop-casting a prepared Ir complex ink ((PNNP)Ir–polypyrrole–Nafion–Vulcan) on a carbon material as visualized in Scheme S2, ESI.† The ratio of (PNNP)Ir–polypyrrole–Nafion–Vulcan was recruited based on the composition of the electrodes previously prepared.[20,25] The morphology of a deposited Ir complex (Fig. 1a, **Mes-IrPPh2**) on a carbon material ([**Mes-IrPPh2**], which denotes [Ir-ink] on the carbon electrode) was obtained using scanning electron microscopy (SEM) images (Fig. 1b). The element mapping images obtained *via* energy-dispersive X-ray spectroscopy (EDS) of the [**Mes-IrPPh2**] revealed a homogeneous distribution of C, P, and Ir on the plain surface, while those of the side view indicated that the **Mes-IrPPh2** complex is concentrated on the outer surface of the carbon material (Fig. S1–S3, ESI†). X-ray photoelectron spectroscopy (XPS) of the [**Mes-IrPPh2**] electrode was further conducted to understand the electronic state of the electrode catalyst. The [**Mes-IrPPh2**] electrode before starting the electroreduction exhibited Ir 4f XPS peaks at 63 and 66 eV (Fig. 1c) assignable to Ir(III) (Fig. S4, ESI†)[26] as the original **Mes-IrPPh2** complex. Fig. 1d shows linear sweep voltammetry (LSV) results for the [**Mes-IrPPh2**] electrode. The small onset potential (E_{on}) of −0.24 V *vs.* RHE revealed how quickly the electrocatalyst initializes catalytic activity at such a low potential.

The initial conditions for electrochemical reduction of CO_2 were examined in a two-compartment cell operated at −0.37 V *vs.* RHE using several different PNNP-type Ir complexes (*ca.* 1.43 μmol of Ir in [Ir-ink]; Table S1, ESI†). Among the Ir complexes, **Mes-IrPPh2** showed the most outstanding performance in achieving high product amounts and selectivity towards carbon products ($HCOO^-$ and CO; 765 μmol) with a high current density (5.49 mA cm^{-2}). The FE for $HCOO^-$ formation reached 86%. The results indicate that introducing a bulky mesityl group and modifying the phosphine substituent of the PNNP ligand significantly enhanced $HCOO^-$ production. Replacing the cyclohexyl (Cy) group with a phenyl (Ph) group further improved selectivity by seemingly facilitating π–π/CH–π

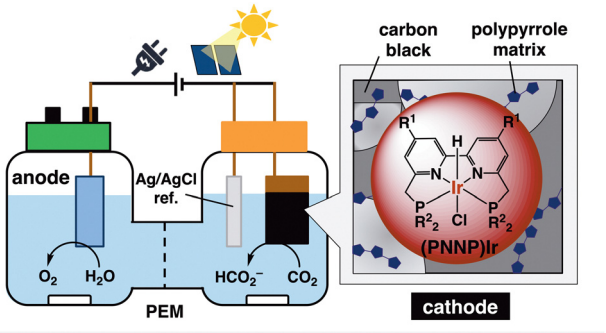

- Electrocatalytic CO_2 reduction at a low overpotential (>90 mV)
- Solar-to-formate conversion efficiency of 13.7%

Scheme 1 Schematic representation of a cell.

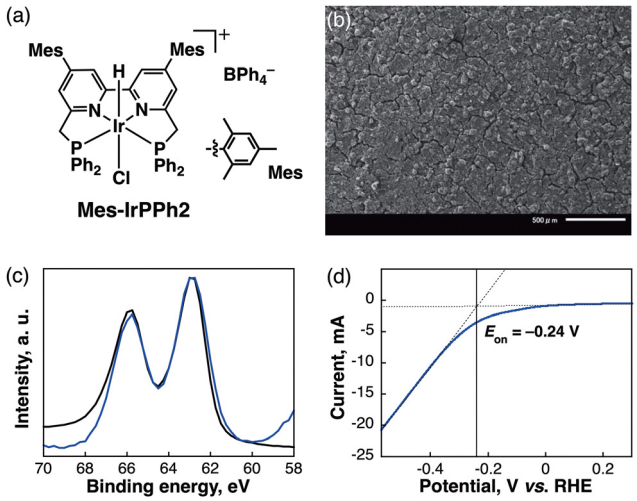

Fig. 1 (a) Chemical structure of **Mes-IrPPh2**. (b) A SEM image of the [**Mes-IrPPh2**] electrode. Scale bar is 500 μm. (c) Ir 4f XPS spectra of the [**Mes-IrPPh2**] (blue line) electrode and $Ir^{III}Cl_3{\cdot}H_2O$ (black line) as a reference. (d) LSV for the [**Mes-IrPPh2**] electrocatalyst in a CO_2-saturated 0.5 M $KHCO_3$ solution.

interactions with the carbon material and polypyrrole. The electrochemical properties of the Ir complexes were recorded using an Ar or CO_2-saturated MeCN solution (Fig. S5, ESI†). Two redox waves were observed for **Mes-IrPPh2** at −0.95 and −1.28 V *vs.* SCE, which were more positive than those of **Mes-IrPCY2** at −1.31 V *vs.* SCE (Fig. S5a, ESI†). When the Ar was replaced by CO_2, the catalytic current with **Mes-IrPPh2** was much enhanced compared to those with **Mes-IrPCY2**, where the E_{on} for **Mes-IrPPh2** (−1.17 V) was also more positive than those of **Mes-IrPCY2** (−1.21 V). The results indicate that subtle modifications in the metal complex ligand structure can have a profound impact on catalytic performance (Fig. S5b, ESI†). The [**Mes-IrPPh2**] electrode operated at a reaction current up to 7.7 mA cm^{-2} over a potential of −0.07 to −0.47 V *vs.* RHE (Fig. 2a), achieving FEs of >90% for $HCOO^-$ production (Fig. 2b and Table S2, ESI†). When the reaction was operated at near-theoretical potential (−0.17 V *vs.* RHE) with a [**Mes-IrPPh2**] electrode, it also produced a miniscule amount of carbon products (18 μmol) with low current density (Fig. 2a, <0.5 mA cm^{-2}). However, it is known that the activation barrier to form $HCOO^-$ can sometimes be overcome by thermal activation at room temperature.[27] To acquire extra energy for inducing the catalyst, the applied potential of −0.27 V *vs.* RHE was selected as an optimum potential in this catalytic system. In the optimized conditions, the lack of each pivotal component (an Ir complex, carbon black, or pyrrole) resulted in the negligible formation of products, while the absence of Nafion gave small amounts of the products at −0.27 V *vs.* RHE for 3 h (Table S3, ESI†). Isotope-labelling experiments using ^{13}C-labeled carbon dioxide ($^{13}CO_2$) in D_2O were conducted to verify the carbon source of the produced $HCOO^-$ and CO. ^{1}H NMR measurement of the reaction solution showed a doublet (J = 194.4 Hz) attributable to the hydrogen atom bound to the ^{13}C atom of $H^{13}COO^-$ (Fig. S6, ESI†). In the ^{13}C NMR spectrum (Fig. S7, ESI†), the formation of $H^{13}COO^-$ was observed together with deuterated formate, $D^{13}COO^-$ (triplet, J = 30.3 Hz).[28] Gas chromatography-mass spectrometry (GC-MS) analysis of the gaseous product also identified ^{13}CO (m/z = 29) as the main gaseous product (Fig. S8, ESI†). The results substantiate that $HCOO^-$ and CO originated from CO_2 rather than from carbon contaminants in the reaction mixture.

The effect of drop-casting (DC) counts of an [Ir ink] on the surface of the working electrode (cathode) was examined to optimize the amounts of the Ir catalyst (Table S4 and Fig. S9, ESI†). By increasing the count of DC from 2 to 4, 6, and 8 times, the amounts of $HCOO^-$ increased at DC = 4 and reached a plateau with DC = 6 or 8, where the current densities continued to rise, ascribable simply to the increased amount of **Mes-IrPPh2** on the electrodes. In all cases, high FEs (>90%) for $HCOO^-$ formation were achieved. Thus, for subsequent experiments, the [**Mes-IrPPh2**] electrodes were prepared using the 4 times DC.

After fabricating the 4 times-DC [**Mes-IrPPh2**] electrode (containing 2.86 μmol of **Mes-IrPPh2**), continuous long-term electrocatalysis of CO_2 at *ca.* −0.27 V *vs.* RHE was conducted over 168 h using a flow reactor for CO_2 supply (Fig. 3a);

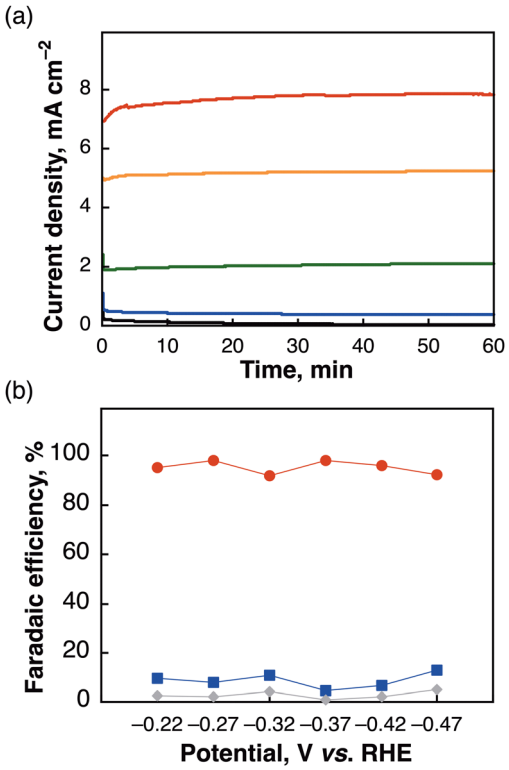

Fig. 2 (a) Chronoamperograms over a [**Mes-IrPPh2**] cathode and a Pt anode for 1 h with several bias voltages [−0.07 V (black), −0.17 V (blue), −0.27 V (green), −0.37 (orange), −0.47 V (red)] and (b) FEs of the products [$HCOO^-$ (red), CO (blue), H_2 (gray)] obtained during the electrocatalytic CO_2 reduction using a [**Mes-IrPPh2**] electrode in a solution of CO_2-saturated 0.5 M $KHCO_3$.

however, the gaseous phase could not be analysed accurately owing to the escaping gas from the reactor. Therefore, we only evaluated the amount of non-gaseous $HCOO^-$ generated in the aqueous phase, which linearly increased over 12.5 mmol with FE of >77% by prolonging the reaction time to 168 h. To ascertain the overwhelming robustness of the [**Mes-IrPPh2**] catalyst, XPS measurements before and after the reaction (3 h, 15 h, and 72 h) were recorded to monitor the reaction of the electrode. The XPS analysis of the Ir 4f region revealed that the Ir metal in **Mes-IrPPh2** was converted from Ir^{III} (Fig. 3b, blue) to Ir^{I} (Fig. 3b, black) within 3 h and the Ir^{I} species remained the same over 72 h (Fig. 3b, red), consistent with the results of ESI-MS analysis (Fig. S10, ESI†). The results indicate that almost no deterioration of the catalyst occurred after an electrolysis for 72 h.

Solar-driven CO_2 reduction was next examined using a two-compartment reactor composed of the [**Mes-IrPPh2**] electrode as a CO_2 reduction catalyst (cathode), Fe/Ni–Ni foam as a water oxidation catalyst (anode),[29] and a heterojunction with an intrinsic thin layer (HIT) solar cell (silicon solar cell), which served as the light absorber with a catalog-specified maximum η_{PV} of approximately 22.7%.[30] A two-compartment reactor separated by a Nafion-117 ion-exchange membrane was used in this system, operating at −2.1 V. The CO_2 reduction using the PV cell was conducted by immersing the cathode–anode

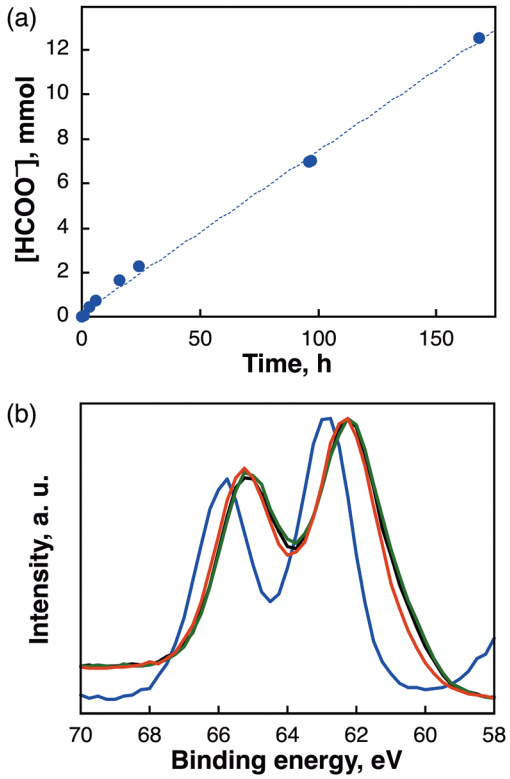

Fig. 3 (a) Time course plots of the $HCOO^-$ obtained during the electrocatalytic CO_2 reduction at −0.27 V *vs.* RHE using a [**Mes-IrPPh2**] cathode and a Pt anode in a solution of CO_2-saturated 0.5 M $KHCO_3$. (b) Ir 4f XPS spectra of a [**Mes-IrPPh2**] electrode [before (blue) and after electrolysis for 3 h (black), 15 h (green), 72 h (red)].

conjunction system in a solution of CO_2-saturated 0.5 M $KHCO_3$ under irradiation with solar simulated light (1 sun, AM1.5) at 308 K. The time course of the FEs for different products is shown in Fig. 4, illustrating that $HCOO^-$ was generated only by the reaction of CO_2 with H_2O as a raw material using sunlight as an energy source. $HCOO^-$ was continuously generated during irradiation for 24 h with over 91% of FEs where CO and H_2 were produced with less than 2% of FEs, respectively, and the solar-to-formate conversion efficiency (η_{STF}) was calculated to be 13.7% from the rate of $HCOO^-$ generation (mmol $HCOO^-$ s^{-1}). It is noteworthy that the η_{STF} up to 13.7% in this system reached the highest level among the photoelectrochemical CO_2 reduction systems[14–20,31] using a molecular catalyst (Table S5, ESI†).

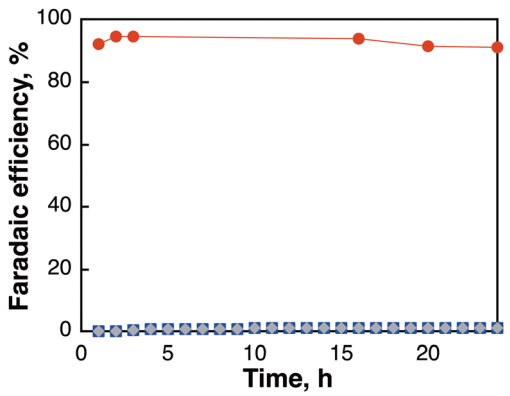

Fig. 4 Time course plots of the product [$HCOO^-$ (red), CO (blue), H_2 (gray)] obtained during the CO_2 electrochemical reduction using a [Mes-IrPPh2] cathode and Fe/Ni–Ni foam anode under simulated solar light irradiation.

Conclusions

In this study, we demonstrated the high-performance systems for electrochemical and solar-driven electrochemical CO_2 reduction in water using a PV cell through the fabrication of an effective cathode deploying a PNNP-type Ir complex as a CO_2 reduction electrocatalyst. The Ir catalyst immobilized on a carbon material ([Ir-ink]: cathode) showed a superior catalytic activity for selective CO_2 reduction to $HCOO^-$, providing FEs of >98% at a constant rate, in addition to an overpotential of no more than ≥90 mV. The rate of production of $HCOO^-$ linearly increased to give 12.5 mmol (using *ca.* 2.86 μmol of Ir) over 168 h at −0.27 V *vs.* RHE, highlighting the extremely robust electrode composed of a (PNNP)Ir complex. The solar-to-formate conversion efficiency of 13.7% was achieved after 24 h irradiation yielding 7 mmol of $HCOO^-$ with FEs of >91%, in conjunction with a Ni/Fe–Ni foam anode as a water oxidation catalyst and a silicon photovoltaic cell as a photon absorber. Through a bespoke molecular design of a robust metal complex with a PNNP ligand backbone, an electrocatalyst made of hybridized molecular catalyst–bulk carbon material promoted $HCOO^-$ formation with concurrent high activity, selectivity, and stability. The present result is in good contrast to the CO_2 reduction systems we have achieved using light energy and C–H bonds (electron and hydrogen donor),[21,22] as well as heat energy and H–H bonds,[32] which were consistently promoted by (PNNP)Ir complex catalysts. This work will surely be further advanced to hitherto unknown efficient solar-driven CO_2 reduction devices using water (O–H bond) as the electron- and hydrogen donor.

Author contributions

Jieun Jung supervised the project on-site and wrote the original draft of the manuscript. Keun Woo Lee, Naonari Sakamoto, and Selvam Kaliyamoorthy conducted the experiments and collected the data. Taku Wakabayashi developed the initial process for solar-driven electrochemical CO_2 reduction. Kenji Kamada provided resources for the research. Keita Sekizawa handled data curation. Shunsuke Sato was responsible for the conceptualization of the study. Tomiko M. Suzuki developed the Fe/Ni–Ni foam as a water oxidation catalyst. Takeshi Morikawa was involved in funding acquisition and administrative aspects. Susumu Saito conceived and supervised the project, managed project administration and funding acquisition, and was responsible for manuscript writing, editing, and curation.

Data availability

The data supporting this article have been included as part of the ESI.†

Conflicts of interest

There are no conflicts to declare.

Acknowledgements

This work was first supported by the Asahi Glass Foundation (step-up grant to S. S.), followed by the Ministry of the Environment of the Government of Japan, and JST CREST (# JPMJCR22L2 to S. S.), Japan. This work was partially supported by a MEXT Grant-in-Aid for Transformative Research Areas (A) Green Catalysis Science (#23H04904 to S. S. and J. J.), a JSPS Grant-in-Aid for Specially Promoted Research (#23H05404 to S. S.), International Leading Research (#22K21346 to S. S.), and an Early-Career Scientist (#21K14642 to J. J.), as well as the Foundation of Public Interest of Tatematsu. We are also grateful to K. Oyama and R. Yamada for their technical support in spectroscopic measurements, K. Higuchi in high voltage electron microscope laboratory for his technical support in SEM/EDS analyses, and H. Natsume, H. Okamoto, and M. Kosaka for their assistance at the custom-made glass workshop.

Notes and references

1 (*a*) J.-P. Jones, G. K. S. Prakash and G. A. Olah, *Isr J. Chem.*, 2014, **54**, 1451–1466; (*b*) S. Garg, M. Li, A. Z. Weber, L. Ge, L. Li, V. Rudolph, G. Wang and T. E. Rufford, *J. Mater. Chem. A*, 2020, **8**, 1511–1544.
2 S. Yoshino, T. Takayama, Y. Yamaguchi, A. Iwase and A. Kudo, *Acc. Chem. Res.*, 2022, **55**, 966–977.
3 A. U. Pawar, C. W. Kim, M.-T. Nguyen-Le and Y. S. Kang, *ACS Sustainable Chem. Eng.*, 2019, **7**, 7431–7455.
4 N. Nandal and S. L. Jain, *Chem. Rev.*, 2022, **451**, 214271.
5 S. A. Al-Tamreh, M. H. Ibrahim, M. H. El-Naas, J. Vaes, D. Pant, A. Benamor and A. Amhamed, *ChemElectroChem*, 2021, **8**, 3207–3220.
6 D. Ewis, M. Arsalan, M. Khaled, D. Pant, M. M. Ba-Abbad, A. Amhamed and M. H. El-Naas, *Sep. Purif. Technol.*, 2023, **316**, 123811.
7 N. Sakamoto, K. Sekizawa, S. Shirai, T. Nonaka, T. Arai, S. Sato and T. Morikawa, *Nat. Catal.*, 2024, **7**, 574–584.
8 Z. Sun, T. Ma, H. Tao, Q. Fan and B. Han, *Chem*, 2017, **3**, 560–587.
9 M. Abdinejad, M. N. Hossain and H.-B. Kraatz, *RSC Adv.*, 2020, **10**, 38013–38023.
10 L. Sun, V. Reddu, A. C. Fisher and X. Wang, *Energy Environ. Sci.*, 2020, **13**, 374–403.
11 P. Kang, S. Zhang, T. J. Meyer and M. Brookhart, *Angew. Chem., Int. Ed.*, 2014, **53**, 8709–8713.
12 X.-M. Hu, M. H. Rønne, S. U. Pedersen, T. Skrydstrup and K. Daasbjerg, *Angew. Chem., Int. Ed.*, 2017, **56**, 6468–6472.
13 S. Sato, K. Saita, K. Sekizawa, S. Maeda and T. Morikawa, *ACS Catal.*, 2018, **8**, 4452–4458.
14 T. Arai, S. Sato, K. Sekizawa, T. M. Suzuki and T. Morikawa, *Chem. Commun.*, 2019, **55**, 237–240.
15 N. Kato, S. Mizuno, M. Shiozawa, N. Nojiri, Y. Kawai, K. Fukumoto, T. Morikawa and Y. Takeda, *Joule*, 2021, **5**, 687–705.
16 N. Kato, Y. Takeda, Y. Kawai, N. Nojiri, M. Shiozawa, S. Mizuno, K. Yamanaka, T. Morikawa and T. Hamaguchi, *ACS Sustainable Chem. Eng.*, 2021, **9**, 16031–16037.
17 X. Chen, H. Chen, W. Zhou, Q. Zhang, Z. Yang, Z. Li, F. Yang, D. Wang, J. Ye and L. Liu, *Small*, 2021, **17**, 2101128.
18 Z. Li, B. Sun, D. Xiao, Z. Wang, Y. Liu, Z. Zheng, P. Wang, Y. Dai, H. Cheng and B. Huang, *Angew. Chem., Int. Ed.*, 2023, **62**, e202217569.
19 X. Chen, J. Chen, H. Chen, Q. Zhang, J. Li, J. Cui, Y. Sun, D. Wang, J. Ye and L. Liu, *Nat. Commun.*, 2023, **14**, 751.
20 T. Nishi, N. Sakamoto, K. Sekizawa, T. Morikawa and S. Sato, *ChemSusChem*, 2024, e202401082.
21 K. Kamada, J. Jung, T. Wakabayashi, K. Sekizawa, S. Sato, T. Morikawa, S. Fukuzumi and S. Saito, *J. Am. Chem. Soc.*, 2020, **142**, 10261–10266.
22 K. Kamada, J. Jung, Y. Kametani, T. Wakabayashi, Y. Shiota, K. Yoshizawa, S. H. Bae, M. Muraki, M. Naruto, K. Sekizawa, S. Sato, T. Morikawa and S. Saito, *Chem. Commun.*, 2022, **58**, 9218–9221.
23 T. Nishi, S. Sato, K. Sekizawa, T. M. Suzuki, K. Oh-ishi, N. Takahashi, Y. Matsuoka and T. Morikawa, *ChemNanoMat*, 2021, **7**, 596–599.
24 S. Yoshioka, S. Nimura, M. Naruto and S. Saito, *Sci. Adv.*, 2020, **6**, eabc0274.
25 T. Arai, S. Sato and T. Morikawa, *Energy Environ. Sci.*, 2015, **8**, 1998–2002.
26 B. van Dijk, G. M. Rodriguez, L. Wu, J. P. Hofmann, A. Macchioni and D. G. H. Hetterscheid, *ACS Catal.*, 2020, **10**, 4398–4410.
27 S. Sato, T. Arai and T. Morikawa, *Nanotechnology*, 2018, **29**, 034001.
28 R. Hudson, R. de Graaf, M. Strandoo Rodin, A. Ohno, N. Lane, S. E. McGlynn, Y. M. A. Yamada, R. Nakamura, L. M. Barge, D. Braun and V. Sojo, *PNAS*, 2020, **117**, 22873–22879.
29 S. Sato, K. Sekizawa, S. Shirai, N. Sakamoto and T. Morikawa, *Sci. Adv.*, 2023, **9**, eadh9986.
30 F. Urbain, P. Tang, N. M. Carretero, T. Andreu, L. G. Gerling, C. Voz, J. Arbiol and J. R. Morante, *Energy Environ. Sci.*, 2017, **10**, 2256–2266.
31 Meanwhile, ηSTF = 14.3% was achieved using an In_2S_3 electrode and an applied voltage of 2.2 V very recently: Q. Zhang, J. Gao, X. Wang, J. Zeng, J. Li, Z. Wang, H. He, J. Luo, Y. Zhao, L. Zhang, M. Grätzel and X. Zhang, *Joule*, 2024, **8**, 1–19.
32 B. Grømer and S. Saito, *Inorg. Chem.*, 2023, **62**, 14116–14123.